CHEMISTRY OF MATERIALS
Article

Chem. Mater. **2010,** *22,* 1977–1987 1977
DOI:10.1021/cm9029038

Cyclometalated Platinum Polymers: Synthesis, Photophysical Properties, and Photovoltaic Performance

Tabitha A. Clem,[†] David F. J. Kavulak,[†,§] Erik J. Westling,[†,§] and Jean M. J. Fréchet*[,†,§]

[†]*College of Chemistry, University of California, Berkeley, California 94720-1460 and* [§]*Materials Sciences Division, Lawrence Berkeley National Laboratory, Berkeley, California 94720*

Received September 17, 2009. Revised Manuscript Received December 1, 2009

The synthesis and characterization of platinum-containing conjugated polymers in which the platinum atom is attached to the conjugated backbone via a *C^N* ligand is presented. The newly designed platinum-containing monomer can be polymerized under both Stille and Suzuki conditions. The polymers exhibit optical bandgaps between 2.1 and 1.65 eV depending on the choice of comonomer. Triplet exciton formation is detected indirectly by measuring photosensitized emission of singlet oxygen in both solution and in film. The ability of the materials to sensitize formation of singlet oxygen varies both with excitation wavelength and with the change from solution to solid state. This study provides design principles for developing conjugated polymers with significant triplet yields in the solid state. The photovoltaic performance of these polymers was also evaluated in preliminary experiments with power conversion efficiencies as high as 1.3% obtained for a bulk heterojunction cell with PCBM.

Introduction

Conjugated polymers with their highly tunable optoelectronic properties and ease of processing[1,2] are interesting materials in the challenging search for efficient low-cost photovoltaic devices. Recently, there has been significant interest in conjugated organometallic polymers as donor polymers for use in bulk heterojunction (BHJ) solar cells in combination with fullerene acceptors.[3−10] In particular, polyplatinynes have drawn some attention as a result of their absorption profiles extending as far as the near-infrared,[10] and their promising charge transport properties with reported hole mobilities as high as 1.0×10^{-2} cm^2 V^{-1} s^{-1} in field-effect transistors (FETs).[9] In addition, polyplatinynes have demonstrated triplet exciton formation.[3,7]

Materials with large triplet yields may well provide access to increased current in organic photovoltaic devices.[11] Triplet excited state lifetimes are typically in the microsecond regime, which is 3 orders of magnitude longer than the nanosecond decays typically observed for singlet excited states in conjugated polymers. Given that exciton diffusion length (L_D) is determined by exciton lifetime (τ) and exciton diffusivity (D) according to the equation $L_D = \sqrt{\tau D}$, a significant increase in lifetime should lead to a longer exciton diffusion length, which would be advantageous for bilayer photovoltaic devices. Triplet-forming polymers have been reported to inhibit geminate pair recombination[3] and to increase the exciton diffusion length[12] in bulk heterojunction devices. However, the conjugated organometallic polymers that have been shown to form triplets in the solid state are also large bandgap systems[12] (>2.5 eV), and therefore power conversion efficiencies are limited by the poor overlap of their absorption spectrum with the solar irradiance. While lower band gap systems have demonstrated formation of triplet excitons in solution, this result does not necessarily translate to the solid state. Furthermore, performance of these lower band gap polymers are limited by charge mobility.[7] It is also important to consider that formation of triplet excitons in a bulk heterojunction device is anticipated to improve the photocurrent primarily by decreasing geminate recombination, as charge separation in a well-mixed bulk heterojunction occurs on the femtosecond time scale[13] while intersystem crossing

*Author to whom correspondence should be addressed: E-mail: frechet@berkeley.edu.

(1) Thompson, B. C.; Fréchet, J. M. J. *Angew. Chem., Int. Ed.* **2008**, *47*, 58–77.
(2) Blom, P. W. M.; M., V. D.; Koster, L. J. A.; Markov, D. E. *Adv. Mater.* **2007**, *19*, 1551–1566.
(3) Guo, F.; Kim, Y.-G.; Reynolds, J. R.; Schanze, K. S. *Chem. Commun.* **2006**, 1887–1889.
(4) Wong, Wai-Yeung *Macromol. Chem. Phys.* **2008**, *209*, 14–24.
(5) Wong, W.-Y.; Wang, X.-Z.; He, Z.; Chan, K.-K.; Djurisic, A. B.; Cheung, K.-Y.; Yip, C.-T.; Ng, A. M.-C.; Xi, Y. Y.; Mak, C. S. K.; Chan, W.-K. *J. Am. Chem. Soc.* **2007**, *129*, 14372–14380.
(6) Wu, P.-T.; Bull, T.; Kim, F. S.; Luscombe, C. K.; Jenekhe, S. A. *Macromolecules* **2009**, *42*, 671–681.
(7) Mei, J.; Ogawa, K.; Kim, Y.-G.; Heston, N. C.; Arenas, D. J.; Nasrollahi, Z.; McCarley, T. D.; Tanner, D. B.; Reynolds, J. R.; Schanze, K. S. *ACS Appl. Mater. Interfaces* **2009**, *1*, 150–161.
(8) Sudha Devi, L.; Al-Suti, M. K.; Zhang, N.; Teat, S. J.; Male, L.; Sparkes, H. A.; Raithby, P. R.; Khan, M. S.; Köhler, A. *Macromolecules* **2009**, *42*, 1131–1141.
(9) Baek, N. S.; Hau, S. K.; Yip, H.-L.; Acton, O.; Chen, K.-S.; Jen, A. K.-Y. *Chem. Mater.* **2008**, *20*, 5734–5736.
(10) Wang, X.-Z.; Wong, W.-Y.; Cheung, K.-Y.; Fung, M.-K.; Djurisic, A. B.; Chan, W.-K. *Dalton Trans.* **2008**, 5484–5494.
(11) Y. Shao, Y. Y. *Adv. Mater.* **2005**, *17*, 2841–2844.
(12) Schulz, G. L.; Holdcroft, S. *Chem. Mater.* **2008**, *20*, 5351–5355.
(13) Moses, D.; Dogariu, A.; Heeger, A. J. *Chem. Phys. Lett.* **2000**, *316*, 356–360.

Published on Web 12/31/2009

occurs in the nanosecond regime.[14] Therefore, in a bulk heterojunction system which has a closely mixed morphology, charge separation will most likely occur before triplet excitons can form. Thus, any improvement in photovoltaic performance for triplet-forming materials in a bulk heterojunction is expected to be primarily the result of decreased geminate recombination or another factor.

In polyplatinynes the poor size and energetic overlap between the 5d Pt and 2p C orbitals leads to a significantly smaller effective conjugation length when compared to structurally analogous poly(phenylene ethynylenes).[15] Given that exciton diffusion length is a function of both lifetime and diffusivity, this exciton localization, or decreased effective conjugation length, may ultimately limit the photovoltaic performance and/or the exciton diffusion lengths observed for these polymers even if long-lived triplets are realized. Organometallic conjugated polymer architectures other than polyplatinynes are therefore worthy of investigation as donor materials to better understand the role of heavy atoms on triplet formation in conjugated polymers for possible application in photovoltaics.

We report a new class of platinum-containing conjugated polymers with optoelectronic properties that are more suitable for photovoltaic applications. These polymers contain a 2-(2′-thienyl)thiazole *C^N* ligand with an *O^O* diketonate ligand that creates a structure analogous to a fused bithiophene system but in which platinum is adjacent to the conjugated backbone and connects the aryl groups into a coplanar conformation. The general structure of these new organometallic polymers is shown in Figure 1. Fused bithiophenes have recently received attention as a building block in low bandgap conjugated polymers, where the optical and electronic properties of the polymer vary with the choice of connecting atom.[16−19] In contrast to the platinum acetylides, the platinum atom is peripheral to the conjugated polymer backbone, leading to a greater involvement from the orbitals of Pt in both the ground and the excited states of the material.[20] This design attempts to minimize any potential decrease in effective conjugation length from the poor overlap of Pt and C orbitals, and creates a platform for the study of the influence of a heavy atom on more diffuse excitons. This design also provides flexibility in tuning the absorption profile and energy levels of the materials simply by varying the Pt ligand and comonomer.

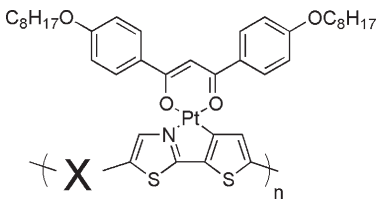

Figure 1. General structure of cyclometalated Pt polymers.

Experimental Section

Synthesis. All chemicals were purchased from commercial sources and used without further purification unless otherwise stated. 2,5-bis(trimethylstannyl)thiophene[21] and 2-(trimethylstannyl)thiophene[22] were prepared as described in the literature. Tetrahydrofuran (THF), *N*,*N*-dimethylformamide (DMF), and toluene were dried by passing through neutral alumina prior to use. All small molecules were characterized by ^{1}H NMR (400 MHz) and ^{13}C NMR (100 MHz) on a Bruker AVB 400 or AVQ 400. Polymer ^{1}H NMR (500 MHz) spectra were obtained on a Bruker DRX 500. All NMR spectra were referenced to TMS. High-resolution mass spectroscopy and elemental analysis (CHN) were performed at the University of California, Berkeley Department of Chemistry analytical services laboratory. IR spectra were recorded on a Varian 3100 FT-IR as KBr pellets or as solid or liquid films drop-cast on KBr discs. Melting points are uncorrected. Column chromatography was performed with silica (230 × 400 mesh). Polymer molecular weights were determined by size exclusion chromatography (SEC) using either dichlorobenzene or THF as the mobile phase as specified. SEC with THF mobile phase (1 mL/min, 45 °C) was carried out using a Waters GPC 150-CV plus system (Milford, MA) with an attached M486 tunable absorbance detector (254 nm), calibrated with polystyrene standards. SEC in dichlorobenzene was performed using HPLC grade dichlorobenzene at a flow rate of 0.8 μL/min on two 300 × 8 mm linear S SDV, 5 μm columns (Polymer Standards Services, USA Inc.) at 70 °C using a Waters (Milford, MA) 2690 separation module and a Waters 486 tunable absorption detector monitored at 350 nm. The instrument was calibrated vs polystyrene standards (1,050 − 135,000 g/mol) and data was analyzed using Millenium 3.2 software.

2-(2′-Thienyl)thiazole (1). 2-(trimethylstannyl)thiophene (1 eq, 6.7 g, 27 mmol) and 2-bromothiazole (1.1 eq, 5.41 g, 33 mmol) were dissolved in anhydrous toluene (240 mL) and anhydrous DMF (60 mL). The solution was degassed by purging with nitrogen for 20 min, then $Pd(PPh_3)_4$ was added under a flow of nitrogen. The solution was kept at 100 °C overnight, then cooled to room temperature and water was added. The aqueous layer was then washed with ether (3 × 100 mL). The organic layers were combined, washed with 1 M HCl three times then dried with anhydrous $NaSO_4$. The solution was filtered and solvent removed to afford an off-white oil. Following purification by column chromatography (SiO_2, 15% EtOAc in hexanes) 4.49 g of the title compound (99% yield) was obtained as a clear oil. ^{1}H NMR (400 MHz, $CDCl_3$) δ 7.76 (d, 1H), 7.50 (dd, 1H), 7.37 (dd, 1 H), 7.22 (d, 1 H), 7.06 (td, 1 H). ^{13}C NMR (100 MHz, $CDCl_3$) δ 162.0, 143.3, 137.3, 127.9, 127.7, 126.6, 118.2. HRMS

(14) Turro, N. J. *Modern Molecular Photochemistry*; University Science Book: Sausalito, CA, 1991; p 628.
(15) Silverman, E. E.; Cardolaccia, T.; Zhao, X.; Kim, K.-Y.; Haskins-Glusac, K.; Schanze, K. S. *Coord. Chem. Rev.* **2005**, *249*, 1491–1500.
(16) Liao, L.; Dai, L.; Smith, A.; Durstock, M.; Lu, J.; Ding, J.; Tao, Y. *Macromolecules* **2007**, *40*, 9406–9412.
(17) Zhou, E.; Nakamura, M.; Nishizawa, T.; Zhang, Y.; Wei, Q.; Tajima, K.; Yang, C.; Hashimoto, K. *Macromolecules* **2008**, *41*, 8302–8305.
(18) Soci, C.; H., I.-W.; Moses, D.; Zhu, Z.; Waller, D.; Gaudiana, R.; Brabec, C. J.; Heeger, A. J. *Adv. Funct. Mater.* **2007**, *17*, 632–636.
(19) Moulé, A. J.; Tsami, A.; Bünnagel, T. W.; Forster, M.; Kronenberg, N. M.; Scharber, M.; Koppe, M.; Morana, M.; Brabec, C. J.; Meerholz, K.; Scherf, U. *Chem. Mater.* **2008**, *20*, 4045–4050.
(20) Brooks, J.; Babayan, Y.; Lamansky, S.; Djurovich, P. I.; Tsyba, I.; Bau, R.; Thompson, M. E. *Inorg. Chem.* **2002**, *41*, 3055–3066.
(21) Van, P. C.; Macomber, R. S.; Mark, H. B.; Zimmer, H. *J. Org. Chem.* **1984**, *49*, 5250–5253.
(22) Rossi, R.; Carpita, A.; Ciofalo, M.; Lippolis, V. *Tetrahedron* **1991**, *47*, 8443–8460.

(EI) calcd. for $C_7H_5NS_2$ 167.9897 found, 167.9891. CHN Calcd. 50.27% C, 3.01% H, 8.37% N, 38.34% S. Found 50.16% C, 3.06% H, 8.24% N, 38.04% S.

5-Bromo-2-(5-bromothiophen-2-yl)-1,3-thiazole (2). 2-(2′-Thienyl)thiazole (1 eq, 7.2 mmol, 1.4 g) was dissolved in 100 mL DMF in an ice bath and treated dropwise with a solution of *N*-bromosuccinimide (2.5 eq, 18 mmol, 3.3 g) in 100 mL DMF. The solution was allowed to warm to room temperature and was stirred overnight. The reaction mixture was poured over ice water, and a white solid was formed. The solution was then extracted with diethyl ether (3 × 100 mL). The combined organic layers were then washed with water (3 × 100 mL). The ether layer was dried with $NaSO_4$, filtered, and the solvent removed to obtain a pale orange solid. This solid was applied to a plug of silica and eluted with 20% ethyl acetate in hexanes to obtain the product as a white solid with mp 118−121 °C in 77% yield (2.1 g). ^{1}H NMR (400 MHz, $CDCl_3$) δ 7.63 (s, 1H), 7.18 (d, 1H), 7.04 (d, 1H). ^{13}C NMR (100 MHz, $CDCl_3$) δ 162.2, 144.7, 138.3, 131.0, 126.9, 116.2, 108.2. HRMS (EI) calcd. for $C_7H_3Br_2NS_2$ 326.8033, found 326.8031. CHN Calcd. 25.87% C, 0.93% H, 4.31% N. Found 25.97% C, 0.83% H, 4.22% N.

(2Z)-3-hydroxy-1,3-bis[4-(octyloxy)phenyl]prop-2-en-1-one (3). To a flame-dried, three-neck flask containing **8** (1 eq, 30 mmol, 7.45 g) and **9** (1 eq, 30 mmol, 7.93 g) was added 1,2-dimethoxyethane (150 mL) via cannula. NaH (5 eq, 150 mmol, 3.6 g) was then added in one portion to the stirred solution kept under a strong flow of nitrogen. Once the spontaneous evolution of bubbles from the reaction ceased, the solution was heated to reflux for 24 h, then cooled to room temperature and slowly added to ice water under rapid stirring. This solution was then extracted with ether three times. The combined organic extracts were dried over $MgSO_4$ and solvent was removed under reduced pressure to yield a pale orange solid. This material was recrystallized from a mixture of THF and methanol to yield an off-white solid **3** melting at 76 −77 °C in 48% yield. ^{1}H NMR (400 MHz,$CDCl_3$) δ 17.25 (s, 1H), 7.99 (d, 4H), 7.0 (d, 4H), 6.77 (1, 1H), 4.07 (t, 4H), 1.89 (m, 4H), 1.51 (m, 4H), 1.36 (m, 16H), 0.94 (t, 6H). ^{13}C (100 MHz, $CDCl_3$) δ 184.57, 162.61, 129.02, 127.88, 114.35, 91.35, 68.23, 31.79, 29.32, 29.21, 29.11, 25.98, 22.64, 14.09. HRMS (FAB) for $C_{31}H_{44}O_4$ calcd. 481.3318, found 481.3323. CHN Calcd. 77.46% C, 9.23% H. Anal. 77.42% C, 9.48% H. IR (KBr Pellet) 2957, 2923, 2855, 2362, 2343, 1545, 1507, 1491, 1472, 1429, 1385, 1308, 1263, 1227, 1174, 1125, 1105, 1064, 1030, 999, 972, 945, 922, 895, 859, 847, 785, 721, 699, 668, 653, 643, 597 cm^{-1}.

Platinum(II) (2-(2′-thienyl)thiazolato-*N*,*C*$^{2'}$) ((2Z)-3-hydroxy-1,3-bis[4-(octyloxy)phenyl]prop-2-en-1-onato-*O*,*O*) (4). Potassium tetrachloroplatinate (0.62 g, 3 mmol, 1 equiv) was dissolved in 60 mL H_2O, and 2-(2′-thienyl)thiazole (0.5 g, 6 mmol, 2 equiv) was dissolved separately in 180 mL ethoxyethanol. The solutions were combined and heated to 90 °C overnight under nitrogen. The solution was then cooled to room temperature and poured over 100 mL of ice-cold water. The dark green precipitate which formed was collected by filtration and washed with water and methanol, then dried under vacuum overnight without further purification (0.456 g). The dried precipitate (1.0 g, 1.8 mmol, 1 equiv) was treated with **3** (2.59 g, 5.4 mmol, 3 equiv) and Ag_2O (0.76 g, 3.33 mmol, 1.85 equiv) in dry, degassed THF (18 mL), and heated to reflux overnight. The reaction mixture was filtered, and the remaining solid was washed extensively with dichloromethane. After removing the solvent, the resulting brown solid was passed through a silica column (CH_2Cl_2). The product collected as the first orange spot was further purified by recrystallization from a mixture of methanol and dichloromethane to yield an orange solid with mp at 131−133 °C (0.76 g, 51% yield). ^{1}H NMR (400 MHz, $CDCl_3$) δ 8.00 (dd, 4H), 7.31 (d, 2H), 7.57 (d, 1H), 7.30 (d, 1H), 7.16 (d, 1H), 6.94 (dd, 4H), 6.71 (s, 1H), 4.02 (t, 4H), 1.82 (q, 4H), 1.49 (m, 4H), 1.34 (m, 16H), 0.91 (t, 6H) ^{13}C NMR (100 MHz, $CDCl_3$) δ 177.74, 176.79, 173.39, 161.48, 146.17, 137.57, 131.97 (d, J = 103 Hz), 129.77 (d, J = 85 Hz), 128.76, 114.24, 113.5, 95.31, 68.17, 31.81, 29.35, 29.23, 29.17, 26.02, 22.65, 14.11. CHN Calcd. 54.27% C, 5.63% H, 1.67% N. Anal. 54.31% C, 5.32% H, 1.38% N. HRMS (FAB) for $C_{38}H_{47}NO_4PtS_2$ calcd. 840.2638, found 840.2637 IR (KBr film) 3097, 3061, 2924, 2850, 2362, 2311, 1604, 1586, 1524, 1492, 1469, 1444, 1380, 1306, 1263, 1229, 1175, 1129, 1007, 940, 902, 882, 841, 784, 740, 703, 609, 614, 549 cm^{-1}.

Platinum(II) (5-bromo-2-(5-bromothiophen-2-yl)-1,3-thiazolato-*N*,*C*$^{2'}$) ((2Z)-3-hydroxy-1,3-bis[4-(octyloxy)phenyl]prop-2-en-1-onato-*O*,*O*) (5). Potassium tetrachloroplatinate (0.45 g, 1.1 mmol, 1 equiv) was dissolved in 20 mL H_2O and 5-bromo-2-(5-bromothiophen-2-yl)-1,3-thiazole (0.7 g, 2.2 mmol, 2 equiv) was dissolved separately in 70 mL ethoxyethanol. The solutions were combined and heated to 90 °C overnight under nitrogen. The reaction mixture was then cooled to room temperature and poured over 90 mL H_2O. A dark green precipitate was collected by filtration, rinsed with water and methanol, then dried under vacuum overnight (0.6 g). It was used in subsequent steps without additional purification. The dried precipitate (1 eq, 1.35 mmol, 1.52 g), **3** (3 eq, 4.05 mmol, 1.97 g), and Ag_2O (1.85 eq, 2.5 mmol, 0.59 g) were dissolved in dry THF (15 mL) and heated to reflux for 24 h. The solution was then cooled to room temperature and solvent removed under reduced pressure. The product was purified using column chromatography (silica, CH_2Cl_2, R_f = 1.0). The solvent was removed and further purification achieved by recrystallizing the obtained solid from a mixture of CH_2Cl_2 and methanol. The product **5** was obtained as a yellow solid with mp 162−165 °C. ^{1}H NMR (400 MHz, $CDCl_3$) δ 7.93 (t, 4H), 7.68 (s, 1H), 7.10 (s, 1H), 6.93 (t, 4H), 6.58 (s, 1H), 4.04 (t, 4H), 1.82 (m, 4H), 1.52 (m, 4H), 1.35 (m, 16H), 0.93 (t, 6H). ^{13}C (100 MHz, $CDCl_3$) δ 177.71, 176.67, 173.37, 161.78 (d, J = 12 Hz), 148.86, 138.16, 134.04 (d, J = 81 Hz), 131.82 (J = 82 Hz), 129.03, 118.50, 114.51, 101.96, 95.54, 68.44, 53.64, 32.06, 29.61, 29.48, 29.45, 26.28, 22.90, 14.34. HRMS (FAB) for $C_{38}H_{45}Br_2NO_4PtS_2$ calcd. 998.0841, found 998.0844. CHN Calcd. 45.7% C, 4.54% H, 1.40% N. Anal. 45.47% C, 4.45% H, 1.38% N. IR (KBr Pellet) 2920, 2853, 2361, 2343, 1605, 1585, 1559, 1524, 1524, 1472, 1426, 1383, 1305, 1264, 1229, 1178, 1132, 1107, 1037, 959, 839, 781, 667, 635, 601, 578 cm^{-1}.

4-Octyloxyacetophenone (8). 4-hydroxyacetophenone (1 eq, 60 mmol. 8.17 g) was dissolved in anhydrous DMF (120 mL) with anhydrous K_2CO_3 (3 eq, 180 mmol, 24.88 g) and 1-bromooctane (1.2 eq, 72 mmol, 13.90 g). The solution was stirred at 60 °C overnight. The reaction was cooled to room temperature, then poured over 100 mL water and extracted into ether (3 × 100 mL). The organic fractions were combined and washed with water three times to remove any remaining DMF. The organic fractions were then dried with $MgSO_4$ and the solvent removed under reduced pressure to yield a brown oil. This oil was flushed through a plug of silica in 10% EtOAc in hexanes to give a pale brown oil. The oil was stirred under vacuum at 60 °C overnight to remove any residual bromooctane. The oil was then placed in the freezer at −20 °C, whereupon it became a solid and remained a solid with mp at 32−35 °C. Yield: 12.89 g, 85%. ^{1}H NMR (400 MHz,$CDCl_3$): δ 7.99 (d, 2H), 6.90 (d, 2H), 4.01 (t, 2H), 2.55 (s, 3H), 1.82 (quintet, 2H), 1.2−1.5 (m, 10H), 0.87 (t, 3H). ^{13}C NMR (100 MHz, $CDCl_3$) δ 196.76, 163.08, 130.54, 130.02,

114.07, 68.21, 31.77, 29.29, 29.19, 29.06, 26.30, 25.95, 22.62, 14.08. HRMS (EI) for $C_{16}H_{24}O_2$ calcd. 248.1776, found 248.1771 CHN Calcd. 77.38% C, 9.74% H. Anal. 77.48% C, 9.96% H. mp 28−31 °C IR (KBr film) 2925, 2856, 2364, 1677, 1601, 1578, 1541, 1509, 1468, 1420, 1357, 1306, 1255, 1171, 1114, 1077, 1019, 955, 834, 814, 725, 590 cm^{-1}.

4-Octyloxy Benzoic Acid Methyl Ester (9). 4-Hydroxybenzoic acid methyl ester (1 eq, 60 mmol, 9.13 g) was dissolved in anhydrous DMF (120 mL) with anhydrous K_2CO_3 (3 eq, 180 mmol, 24.88 g) and 1-bromooctane (1.2 eq, 72 mmol, 13.90 g) and stirred at 60 °C overnight. The reaction was cooled to room temperature, then water and ether were added. The organic layer was washed three times with water to remove any remaining DMF. The organic fractions were then dried with $MgSO_4$ and the solvent removed to give an off-white solid. This solid was applied to a silica column and eluted with 10% EtOAc in hexanes. Recrystallization from ethanol afforded a white solid with mp 35−36 °C. Yield: 12.0 g, 76%. ^{1}H NMR (400 MHz, $CDCl_3$): δ 7.99 (d, 2H), 6.91 (d, 2H), 3.98 (t, 2H), 3.88 (s, 3H), 1.77 (m, 2H), 1.49 (m, 2H), 1.32 (m, 8H), 0.89 (t, 3H). ^{13}C (100 MHz, $CDCl_3$) δ 167.11, 163.16, 131.75, 122.49, 114.24, 68.39, 52.00, 32.00, 29.52, 29.42, 29.31, 26.18, 22.85, 14.29. HRMS (EI) for $C_{16}H_{24}O_3$ calcd. 265.1759, found 265.1761 CHN Calcd. 72.69% C, 9.15% H. Anal. 72.85% C, 9.38% H. IR (KBr disk) 2929, 2857, 1721, 1610, 1607, 1579, 1512, 1469, 1435, 1394, 1315, 1280, 1255, 1169, 1105, 1023, 972, 847, 771, 697, 648 cm^{-1}.

Pt-T1. To a flame-dried three neck flask was added **5** (1 eq., 0.100 g, 0.100 mmol) and 5 mL anhydrous THF and the solution was treated with 2,5-bis(trimethylstannyl)-thiophene (1 eq, 0.041 g, 0.100 mmol). The solution was stirred, purging with nitrogen for 20 min. Following degassing, $Pd(P^tBu_3)_2$ (0.02 eq, 1 mg, 0.002 mmol) and CsF (4 eq, 0.060 g, 0.402 mmol) were added quickly under strong flow of nitrogen. The solution was then stirred and heated to 40 °C overnight. After 24 h, the solution was cooled to room temperature and precipitated into methanol. The crude polymer was recovered by filtration and further purified by Soxhlet extraction with methanol, chloroform, and chlorobenzene. The chlorobenzene fraction was concentrated and reprecipitated into methanol to obtain 29 mg (32% yield) of polymer free of low molecular weight material.

^{1}H NMR (500 MHz, $C_2D_2Cl_2$, 90 °C) δ 6.5−8.0 (br, 13H), 3.96 (br, 4H), 0.5−2.0 (br, 30H). CHN Calcd. 54.77% C, 5.14% H, 1.52% N, 10.44% S. Anal. 51.66% C, 5.49% H, 1.51 N, 9.29% S. SEC (dichlorobenzene) M_n 45 kDa, M_w 84 kDa, PDI 1.9 IR (KBr Pellet) 2923, 2849, 2366, 2344, 1602, 1585, 1528, 1490, 1472, 1418, 1384, 1303, 1256, 1227, 1173, 1132, 1108, 1022, 969, 954, 837, 779, 667, 653, 630, 561, 519 cm^{-1}.

F8TZPt. To a three-neck flask was added **5** (1 eq, 0.060 g, 0.060 mmol) and 9,9-dioctylfluorene-2,7-bis(trimethylborate) (1 eq, 0.032 g, 0.06 mmol), and potassium fluoride (3.3 eq, 0.012 g, 0.198 mmol). THF (3 mL) and H_2O (1 mL) were added and the solution purged with nitrogen for 20 min. $Pd(P^tBu_3)_2$ (0.08 eq, 0.02 g, 0.004 mmol) and Pd_2dba_3 (0.04 eq, 0.02 g, 0.002 mmol) were added under strong flow of nitrogen and the solution was stirred at 40 °C for 24 h. After 24 h the solution was precipitated into methanol, and then purified by Soxhlet extraction with methanol, then chloroform. The chloroform fraction was concentrated and reprecipitated into methanol to obtain 54 mg of polymer (73% yield). ^{1}H NMR (500 MHz, $CDCl_3$) δ 8.0−8.5 (br, 5H), 7.3−7.9 (m, 6H), 6.6−7.2 (m, 6H), 4.1 (s, 4H), 1.7−2.4 (br, 8H), 1.0−1.5 (m, 38H), 0.5−1.0 (m, 18H). CHN Calcd. 65.44% C, 7.13% H, 1.14% N. Anal. 61.32% C, 6.93% H, 1.12 N. SEC (THF) M_n 24 kDa, M_w 47 kDa, PDI 1.9. IR (KBr film) 2956, 2925, 2854, 2365, 1674, 1604, 1586, 1527, 1492, 1467, 1425, 1383, 1305, 1259, 1229, 1175, 1134, 1093, 1024, 841, 801, 725 cm^{-1}.

Optical and Electrochemical Measurements. Cyclic voltammetry (CV) was performed using a Solartron 1285 potentiostat. For the polymers, CV was performed on thin films dip-coated onto a Pt wire working electrode and submerged in CH_3CN freshly distilled from CaH_2. For small molecules, the cyclic voltammograms were measured in dichloromethane solution with a Pt wire working electrode. All measurements were performed using a silver wire pseudoreference electrode, a platinum auxiliary electrode, and were referenced to the ferrocene/ferrocenium couple, which was taken to be −5.1 eV relative to vacuum.[23] Tetrabutylammonium tetrafluoroborate (NBu_4BF_4) was the supporting electrolyte for all measurements. UV−visible absorption spectra were obtained using a Cary 50 UV−visible spectrophotometer. For thin film measurements polymers were spin coated onto untreated glass slides from chlorobenzene solution (10 mg mL^{-1}). A model P6700 Spincoater was used to spin coat the films at 1500 rpm for 60 s. Photoluminescence spectra were obtained using a Horiba Jobin Yvon Nanolog fluorimeter. For deoxygenated samples, the solvent was degassed by three freeze−pump−thaw cycles, and then the solutions were freshly prepared inside of a glovebox under argon atmosphere. For aerated samples, the solution was purged with air for 5 min prior to measurement.

Device Fabrication and Measurement. Photovoltaic devices consisted of a standard ITO/PEDOT:PSS/Pt-polymer:PCBM/Al architecture. Indium-doped tin oxide (ITO) coated glass substrates were purchased from Thin Film Devices, Inc. The substrates (150 nm sputtered pattern, 10 $\Omega\,\square^{-1}$) were cleaned by 20 min of sonication in acetone, 2% Helmanex soap in water, and finally isopropanol. The substrates were then dried under a stream of air before being coated immediately with a filtered (0.45 μm GHP) dispersion of PEDOT:PSS in water (Baytron-PH) via spin coating for 30 s at 4000 rpm. The resulting polymer layer was ~30 nm thick after baking at 140 °C for 20 min. All subsequent device fabrication was performed inside a glovebox under inert Ar atmosphere with water and oxygen levels below 1 ppm. Each Pt-polymer was dissolved at a concentration of 16 mg mL^{-1} in chlorobenzene. PCBM (purchased from Nano-C) was dissolved separately at 40 mg mL^{-1} in chlorobenzene and all solutions were allowed to stir overnight at 120 °C. The solutions were then combined in various ratios from 1:1 to 1:6 polymer:PCBM along with additional chlorobenzene as needed to a final polymer concentration of 8 mg mL^{-1}, before spin-casting onto the PEDOT:PSS-treated ITO at 1200 rpm for 30 s. 100 nm aluminum electrodes were deposited by thermal resistance evaporation at pressures of approximately 10^{-6} torr to complete the device structure. The shadow mask used during thermal deposition yielded eight independent devices per substrate each with a surface area of 0.03 cm^2. Completed devices were then tested under Ar(g) using a 300 W Thermo-Oriel Xenon arc-lamp with flux control spectrally corrected to AM 1.5 G with one filter (Thermo-Oriel No. 81088). The AM 1.5 G light was further attenuated using a 0.5 O.D. neutral density filter, and the intensity of the AM 1.5 G light was calibrated to be 100 mW cm^{-2} by a spectrally matched Hamamatsu S1787−04 photodiode (calibrated by NREL and obtained through Nanosys Inc.). I−V behavior was measured using a computer-controlled Keithley 236 SMU.

(23) Pavlishchuk, V. V.; Addison, A. W. *Inorg. Chim. Acta.* **2000**, *298*, 97–102.

Scheme 1. Synthesis of Monomer and Model Complex

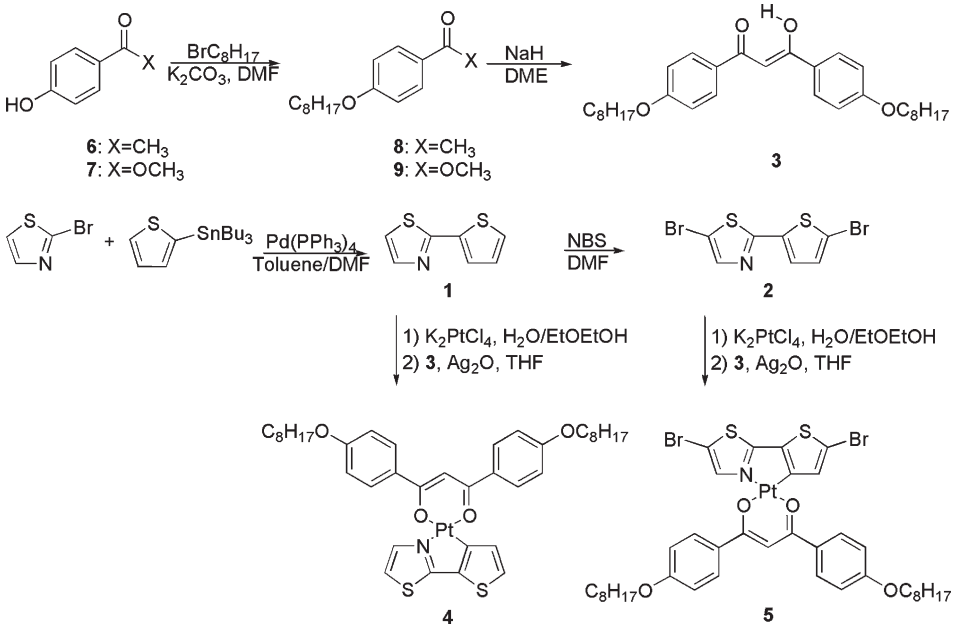

Polymer mobility was measured using a diode configuration of ITO/PEDOT:PSS/Polymer/Al in the space charge limited current regime. At sufficient potential the conduction of charges in the device can be described by

$$J_{\mathrm{SCLC}} = \frac{9}{8}\varepsilon_r\varepsilon_0\mu\frac{V^2}{L^3} \quad (1)$$

where ε_0 is the permittivity of space, ε_R is the dielectric of the polymer (assumed to be 3), μ is the mobility of the majority charge carriers, V is the potential across the device ($V = V_{\mathrm{applied}} - V_{\mathrm{bi}} - V_{\mathrm{r}}$), and L is the polymer layer thickness. The series and contact resistance of the device (13−21 Ω) was measured using a blank (ITO/PEDOT/Al) and the voltage drop due to this resistance (V_{r}) was subtracted from the applied voltage. The built-in voltage (V_{bi}), which is based on the relative work function difference of the two electrodes, was also subtracted from the applied voltage. The built-in voltage can be estimated from the difference in work function between the cathode and anode and is found to be about 1 V.

Results and Discussion

Synthesis. The new Pt-containing dibrominated monomer **5** was synthesized as shown in Scheme 1, using a modification of the procedure of Venkatesan et al.[24] In order to take advantage of the high photovoltaic efficiencies,[25,26] high charge carrier mobilities[27] and strong light absorption[28] associated with polythiophenes, we chose the 2-(2′-thienyl)thiazole *C^N* ligand which also contains a thiophene. The thiazole unit should also contribute favorably to charge mobility[29,30] while providing a nitrogen atom for Pt coordination and minimizing donor−acceptor interactions in the polymer. The diphenyl ketonate ligand provides solubility via the peripheral dialkoxy groups. Since platinum complexes containing the 2-(2′-thienyl)thiazole ligand have not been reported previously, model complex **4** without terminal bromine moieties was synthesized to enable a comparison of optical and electronic properties of the repeat unit to those of the corresponding polymers. Stille and Suzuki polymerizations were carried out using $Pd(P^tBu_3)_2$, and conditions were based on those developed by the Fu group,[31,32] as shown in Scheme 2. This palladium system was used in place of the $Pd(PPh_3)_4$ analog, because compound **5** was found to degrade under polymerization conditions using the more classical catalyst. This degradation was confirmed by significant changes to the ^{1}H NMR spectrum of **5** after adding a solution of PPh_3. The exact nature of this degradation is unknown, but $Pt(acac)_2$ complexes have been shown to react with triaryl phosphine ligands by displacing one of the O atoms of the diketonate ligand[33] or by forming a pentacoordinate complex.[34] The tri(*tert*-butyl)phosphine ligand is significantly more bulky than triphenylphosphine, as evidenced by its ability to form a stable divalent Pd(0) complex at room temperature,[32] and by its larger cone angle of 182° versus the 145° determined

(24) Venkatesan, K.; Kouwer, P. H. J.; Yagi, S.; Muller, P.; Swager, T. M. *J. Mater. Chem.* **2008**, *18*, 400–407.
(25) Hou, J.; Chen, H.-Y.; Zhang, S.; Li, G.; Yang, Y. *J. Am. Chem. Soc.* **2008**, *130*, 16144–16145.
(26) Lee, J. K.; Ma, W. L.; Brabec, C. J.; Yuen, J.; Moon, J. S.; Kim, J. Y.; Lee, K.; Bazan, G. C.; Heeger, A. J. *J. Am. Chem. Soc.* **2008**, *130*, 3619–3623.
(27) Chua, L.-L.; Zaumseil, J.; Chang, J.-F.; Ou, E. C. W.; Ho, P. K. H.; Sirringhaus, H.; Friend, R. H. *Nature* **2005**, *434*, 194–199.
(28) Kim, Y.; Cook, S.; Tuladhar, S. M.; Choulis, S. A.; Nelson, J.; Durrant, J. R.; Bradley, D. D. C.; Giles, M.; McCulloch, I.; Ha, C.-S.; Ree, M. *Nat. Mater.* **2006**, *5*, 197–203.
(29) Hong, X. M.; Katz, H. E.; Lovinger, A. J.; Wang, B.-C.; Raghavachari, K. *Chem. Mater.* **2001**, *13*, 4686–4691.
(30) Li, W.; Katz, H. E.; Lovinger, A. J.; Laquindanum, J. G. *Chem. Mater.* **1999**, *11*, 458–465.
(31) Littke, A. F.; Dai, C.; Fu, G. C. *J. Am. Chem. Soc.* **2000**, *122*, 4020–4028.
(32) Littke, A. F.; Schwarz, L.; Fu, G. C. *J. Am. Chem. Soc.* **2002**, *124*, 6343–6348.
(33) Okeya, S.; Miyamoto, T.; Ooi, S. I.; Nakamura, Y.; Kawaguchi, S. *Inorg. Chim. Acta.* **1980**, *45*, L135–L137.
(34) Ooi, S. I.; Matsushita, T.; Nishimoto, K.; Okeya, S.; Nakamura, Y.; Kawaguchi, S. *Bull. Chem. Soc. Jpn.* **1983**, *56*, 3297–3301.

Scheme 2. Synthesis of Polymers

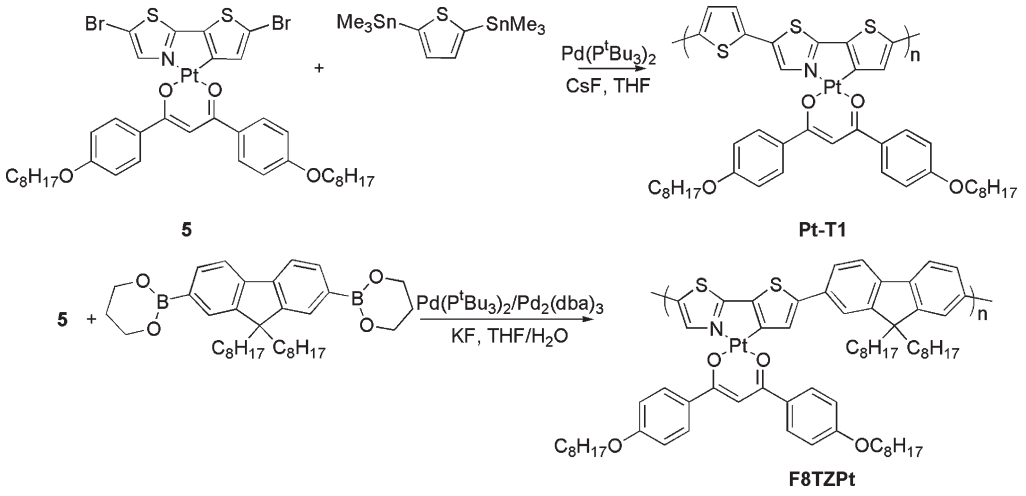

Table 1. Molecular Weights of Polymers Studied

polymer	Mn	M_w	PDI
Pt-T1[a]	45 kDa	84 kDa	1.9
F8TZPt[b]	24 kDa	47 kDa	1.9

[a] SEC in Dichlorobenzene. [b] SEC in THF (both calibrated with polystyrene standards).

for triphenylphosphine.[35] This bulkiness likely hinders coordination of the ligand on the Pt center of **5**, allowing the polymerization to proceed without disturbance to the metal complex. In addition, the high activity of the $Pd(P^tBu_3)_2$ catalyst system makes it possible to achieve high molecular weight polymers via both Stille and Suzuki coupling routes at 40 °C, a lower reaction temperature than the 80−100 °C frequently used for analogous Pd-catalyzed polymerizations. The reduced reaction temperature should also contribute to the improved stability of the platinum complex during polymerization.

The crude polymers were isolated by precipitation into methanol, followed by Soxhlet extraction with methanol and hexanes to remove low molecular weight impurities, and finally chloroform or chlorobenzene to collect the desired polymer fraction. The chlorobenzene fraction of **Pt-T1** and the chloroform fraction of **F8TZPt** were isolated and reprecipitated into methanol for further study. As shown in Table 1, monomer **5** is an excellent monomer for the preparation of a variety of Pt-containing polymers via Stille or Suzuki protocols affording high molecular weight soluble polymers. ^{1}H NMR and FT-IR analysis of the polymers indicated that the platinum complex remains intact after polymerization.

Optical and Electronic Properties. The optical and electronic properties of **4**, **F8TZPt**, and **Pt-T1** were studied to determine the suitability of these materials for photovoltaic applications, and to further understand the effects of extending conjugation through a cyclometalated platinum complex. Figure 2a shows the UV−vis absorbance spectra for **4**, **Pt-T1**, and **F8TZPt** in dilute chloroform solution and Figure 2b shows the UV−vis

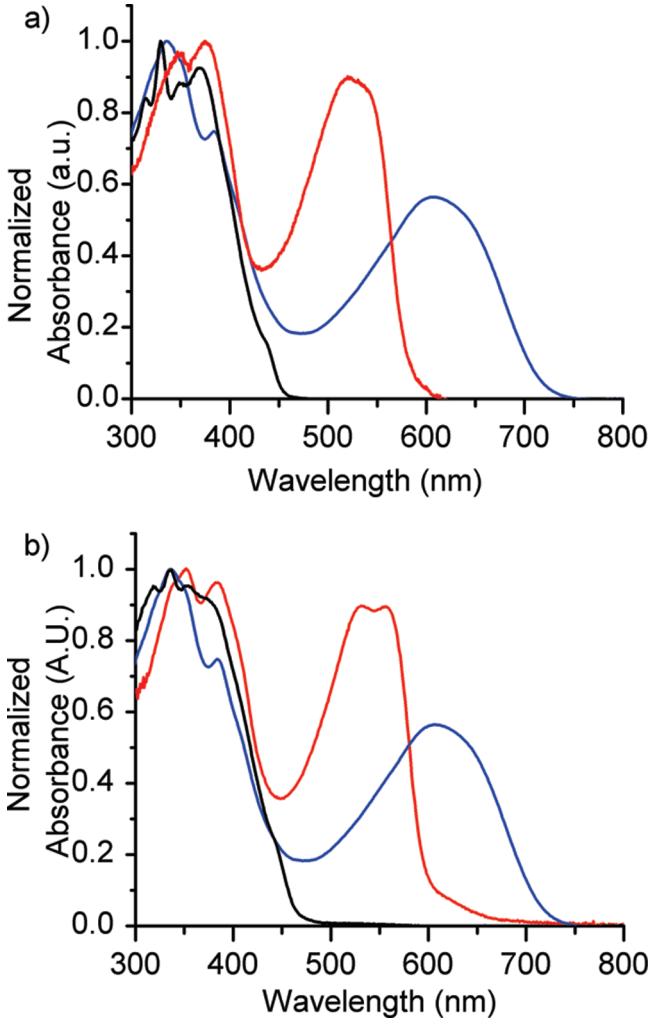

Figure 2. Overlaid absorption spectra of polymers and small molecule in chloroform solution (a) and thin film (b): **4** (black), **Pt-T1** (blue), and **F8TZPt** (red).

absorbance spectra for **4, Pt-T1** and **F8TZPt** in thin films. Both polymers exhibit a strong transition at approximately 350 nm, which, given the similarity between this peak and the absorption profile of the small molecule **4,** is attributed to the direct excitation of the metal complex.

(35) Tolman, C. A. *Chem. Rev.* **1977**, *77*, 313–348.

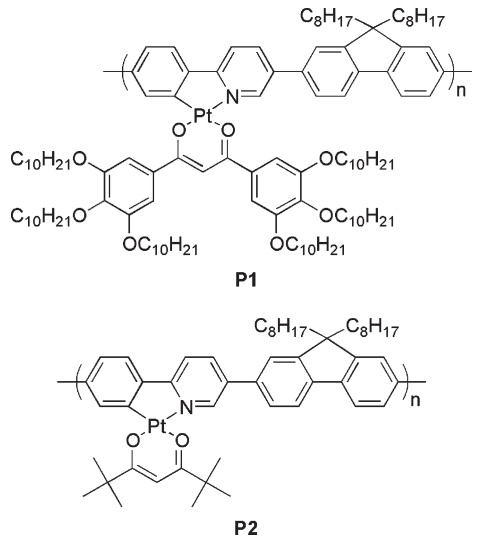

Figure 3. Previously reported platinum-containing polyfluorenes.[36]

Both polymers also show strong transitions at longer wavelengths, with peaks at 610 and 520 nm for solutions of **Pt-T1** and **F8TZPt**, respectively. These peaks are attributed to excitations delocalized along the conjugated polymer chain. The absorption for **F8TZPt** is significantly red-shifted when compared to those of the previously reported platinated polyfluorenes **P-1** and **P-2** shown in Figure 3.[36]

Changing the *C^N* ligand in the fluorene copolymers from 2-phenylpyridine in **P1** or **P2** to 2-(2′-thienyl)thiazole in **F8TZPt** causes the lower energy absorption maximum to shift from 450 nm[36] to 520 nm. The small molecule complexes containing 2-phenylpyridine[20] and 2-(2′-thienyl)-thiazole have similar absorption spectra, so this larger bathochromic shift suggests that **F8TZPt** may have significant donor−acceptor character. Further, these results show that the optical properties of these platinum-containing polymers can be tuned by modifying either or both the platinum complex and the comonomer. The UV−vis spectrum of **F8TZPt** also exhibits a redshift from 520 to 555 nm when changing from solution to film. This shift in absorption to longer wavelengths together with the enhanced vibronic structure is indicative of increased $\pi-\pi$ stacking in the solid state. In contrast, the spectrum for **Pt-T1** broadens and redshifts slightly going from solution to the solid state, but does not exhibit vibronic structure. Based on the onset of absorption in the solid state, the optical bandgap of **F8TZPt** is 2.1 eV. The optical bandgap of **Pt-T1** is 1.65 eV, close to the theoretically ideal bandgap of 1.5 eV for a donor material in a polymer: PCBM solar cell.[18]

In addition to the absorption properties, the HOMO and LUMO of the donor material are key parameters that influence the overall performance of a photovoltaic device by affecting the efficiency of charge separation and the maximum attainable open-circuit voltage (V_{OC}). Cyclic voltammograms (CV) of **Pt-T1**, **F8TZPt**, and **4** were used to determine their oxidation and reduction potentials. The HOMO level was determined by the onset of oxidation, the LUMO was determined by the onset of reduction when it was observed and determined by the difference between the HOMO and the optical bandgap. The oxidations and reductions observed were all irreversible, which is consistent with previously reported Pt(II) complexes.[37] For the small molecule **4** no reduction peak was observed, but an irreversible oxidation was observed at 0.3 V corresponding to a HOMO of −5.4 eV. This HOMO level is comparable to that of the *C^N* ligand **1**, which has a HOMO of −5.3 eV, suggesting that the HOMO of the platinum complex is primarily based on the *C^N* ligand. The polymer **Pt-T1** undergoes an irreversible oxidation at −5.4 eV, and an irreversible reduction at −3.5 eV, for an electrochemical bandgap of 1.9 eV. The optical bandgap for **Pt-T1** is slightly smaller (1.65 eV). However for **F8TZPt** the HOMO is lower at −5.6 eV. The HOMO of poly(9,9-dioctyfluorene) (PFO) is −5.7 eV,[27] suggesting that the HOMO of **F8TZPt** is at least partly influenced by the fluorene moiety. An electrochemical reduction was not observed for **F8TZPt**, but based on the difference between the optical bandgap and the HOMO, the LUMO is estimated to be −3.5 eV. The optical and electronic properties of all the materials are summarized in Table 2. Taken together the data indicate that both the optical bandgap and the HOMO levels of the materials may be tuned by varying the comonomer, whereas the LUMO is primarily determined by the platinum complex.

Photoluminescence and Singlet Oxygen Generation. Organometallic conjugated polymers with large intersystem crossing yields have demonstrated increased photocurrent in photovoltaic devices. This increase in performance has been attributed to decreased geminate recombination[3] and increased exciton diffusion length due to the forbidden nature of recombination from the triplet state.[12] However, these previously reported polymers have bandgaps larger than 2.5 eV, resulting in poor overlap with the solar spectrum. The polymers presented here absorb strongly in the visible spectrum; they are also expected to possess more delocalized excitons than the polyplatinynes, providing a new platform to study the effect of a heavy atom on intersystem crossing in conjugated polymers.

To investigate the influence of the Pt center on the **F8TZPt** and **Pt-T1** polymers the emission spectra of all materials (including monomer precursors) were measured at both long and short excitation wavelengths. All experiments were conducted in degassed benzene solution. At room temperature, **4** exhibits a phosphorescence peak with an onset at 575 nm (2.16 eV) and a maximum at 660 nm when excited at 370 nm. This peak can be assigned to a $T_1 \rightarrow S_0$ transition as evidenced by the large Stokes shift and long lifetime (3.8 μs). The triplet energy of the small molecule is at a lower energy relative than reported for several other *C^N*Pt(*O^O*) complexes, which is most

(36) Thomas, S. W. Y., S.; Swager, T. M. *J. Mater. Chem.* **2005**, *15*, 2829–2835.

(37) Kvam, P.-I. P.; Michael, V.; Balashev, Konstantin P.; Songstad, Jon. *Acta Chem. Scand.* **1995**, *49*, 335–343.

Table 2. Optical and Electronic Properties

sample	λ_{max}, $CHCl_3$ solution	λ_{onset}, film	E_g optical (eV)	HOMO (eV)	LUMO[a] (eV)	LUMO[b] (eV)
4	330 nm	475 nm	2.6	−5.4	N/A	−2.8
Pt-T1	335 nm, 610 nm	750 nm	1.65	−5.4	−3.5	−3.75
F8TZPt	375 nm, 520 nm	600 nm	2.1	−5.6	N/A	−3.5

[a] Determined by onset of reduction. [b] Estimated according to LUMO=HOMO-E_g optical.

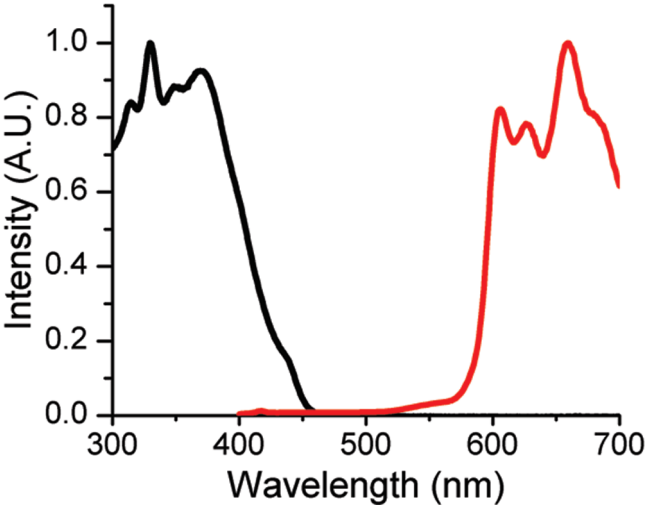

Figure 4. Absorbance and emission of **4**: absorbance (black) and emission (red).

likely due to the electron rich nature of the *C^N* and *O^O* ligands.[20] Further, the triplet energy of the complex is above the triplet energy of poly(3-octylthiophene) (1.65 eV) and below that of PFO (2.3 eV),[38] suggesting that in **Pt-T1** energy transfer from the triplet of the complex to the triplet of the polymer may readily occur. Conversely, energy transfer from the metal complex may be disfavored for the fluorene copolymer **F8TZPt**. The absorbance and photoluminescence of **4** are shown in Figure 4.

The observed phosphorescence of the complex at room temperature is in sharp contrast to the reported behavior[36] of other diphenyl ketonate-substituted platinum complexes, which show no emission from the triplet state as a result of the thermal equilibrium between the *C^N* ligand-centered (^{3}LC) emissive state and the nonemissive Pt/diphenyl ketonate charge transfer (^{3}CT) state.[36] The significant phosphorescence from **4** at room temperature indicates that the triplet state of **1** lies sufficiently below the triplet state of the diphenyl ketonate to inhibit this nonradiative decay pathway. At room temperature, degassed solutions of both polymers **F8TZPt** and **Pt-T1** show weak emission with small Stokes shifts suggesting emission from the singlet state. Although phosphorescence is not observed for **Pt-T1** or **F8TZPt**, they may still undergo intersystem crossing to the triplet state followed by nonradiative decay back to the ground state.[39] The weak fluorescence that is observed suggests that another decay pathway, possibly via intersystem crossing, may be more favorable.

Table 3. Singlet Oxygen Generation by Polymers and Model Complex

sample	$\lambda_{excitation}$	singlet oxygen generation
4[a]	370 nm	yes
Pt-T1[a]	370 nm	no
Pt-T1[a]	665 nm	no
Pt-T1[b]	370 nm	yes
Pt-T1[b]	665 nm	no
F8TZPt[a]	370 nm	yes
F8TZPt[a]	530 nm	yes

[a] C_6H_6 solution. [b] 2:1 C_6H_5Cl:C_6H_6 solution.

In order to probe the formation of triplets before nonradiative decay, the ability of both solutions and films of these materials to generate singlet oxygen was explored as a function of excitation wavelength. The efficiency of singlet oxygen photosensitization is strongly correlated to triplet quantum yield in conjugated polymers.[38] Molecular oxygen is able to quench triplet excited states by a variety of energy transfer pathways, leading to luminescence of singlet oxygen that is readily detected at 1270 nm.[40] The results of these experiments are summarized in Table 3.

At room temperature, an aerated benzene solution of **4** shows strong singlet oxygen emission when excited at 370 nm. In contrast, a benzene solution of **Pt-T1** does not sensitize singlet oxygen formation at either short or long excitation wavelengths. Because the sample of **Pt-T1** used in these studies was isolated from chlorobenzene, aggregation of the polymer in a weaker solvent such as benzene was thought to be responsible for quenching. Aggregation of conjugated polymers has been shown to quench excitons via an energy transfer process occurring on a picosecond time scale,[41] faster than the nanosecond time scale typical for intersystem crossing. Indeed, singlet oxygen formation was observed upon excitation at 370 nm when a more strongly solvating 2:1 mixture of chlorobenzene and benzene was used to dissolve **Pt-T1**. The solvent dependence for singlet oxygen generation using **Pt-T1** as a sensitizer indicates that **Pt-T1** is most likely aggregated in pure benzene solution. However, when excited at 665 nm, no singlet oxygen generation is observed from **Pt-T1** even in the better solvent system. Excitation of **Pt-T1** at 370 nm is analogous to excitation of **4**, which quickly undergoes intersystem crossing due to the proximity of the heavy Pt atom and the strong orbital overlap with Pt orbitals in the excited state. Therefore

(38) Burrows, H. D.; Melo, J. S. d.; Serpa, C.; Arnaut, L. G.; Monkman, A. P.; Hamblett, I.; Navaratnam, S. *J. Chem. Phys.* **2001**, *115*, 9601–9606.
(39) Rachford, A. A.; Goeb, S.; Castellano, F. N. *J. Am. Chem. Soc.* **2008**, *130*, 2766–2767.
(40) Schweitzer, C.; Schmidt, R. *Chem. Rev.* **2003**, *103*, 1685–1758.
(41) Fakis, M.; Anestopoulos, D.; Giannetas, V.; Persephonis, P. *J. Phys. Chem. B* **2006**, *110*, 24897–24902.

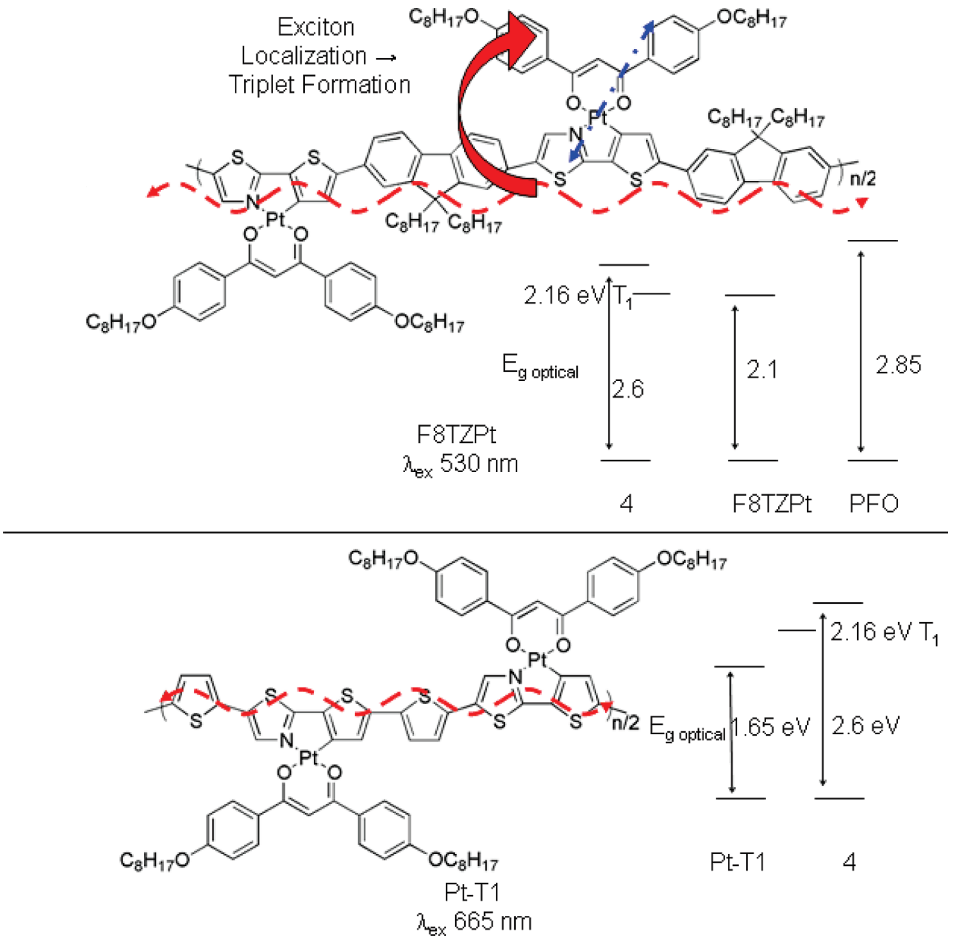

Figure 5. The different means of promotion and inhibition of triplet formation in **F8TZPt** and **Pt-T1** for long wavelength excitations.

triplet formation is facile when exciting at 370 nm. Exciting at 665 nm corresponds to more delocalized excitations that are spread along the polymer backbones. This more delocalized excitation clearly does not exhibit enhanced intersystem crossing. As the exciton becomes more delocalized, the Pt atomic orbitals are expected to make a proportionally smaller contribution to the molecular orbitals associated with the exciton. Given that the singlet energy of **Pt-T1** is lower in energy than the triplet energy of **4**, it is expected that the singlet of **Pt-T1** will not undergo significant energy transfer to the triplet of **4**. Further, it is anticipated that nonradiative decay rates increase relative to the intersystem crossing rate as excitons become more delocalized in a conjugated material.[42]

Benzene solutions of **F8TZPt** exhibit singlet oxygen emission at 1270 nm when excited at either 370 nm or at 530 nm. As was the case for **Pt-T1**, excitation at 370 nm is attributed to excitation of the small molecule chromophore, which rapidly undergoes intersystem crossing. In contrast to **Pt-T1**, **F8TZPt** also generates triplet excitons at longer excitation wavelength. For **F8TZPt**, the initially delocalized exciton may ultimately localize to the platinum moiety because the platinum repeat unit is lower in energy than poly(9,9-dioctylfluorene)[43] as evidenced by their relative energy levels. The singlet energy of **F8TZPt** is close in energy to the triplet energy of 4, suggesting that energy transfer from the singlet of **F8TZPt** to the triplet of **4** can occur readily. This more localized exciton exhibits strong spin−orbit coupling through the platinum atom, leading to formation of triplet excitons as evidenced by sensitized formation of singlet oxygen. The difference in triplet formation observed between **F8TZPt** and **Pt-T1** at long excitation wavelength is illustrated schematically in Figure 5. Red dashed lines represent the excitons initially formed at long excitation wavelengths, with energy transfer occurring to the monomer unit of **4** in the case of **F8TZPt**.

While both polymers are able to sensitize formation of singlet oxygen in solution, neither polymer was observed to sensitize singlet oxygen formation in a thin film. The difference in triplet formation from solution to solid phase, as evidenced by singlet oxygen generation, most likely arises as the result of intermolecular interactions providing a faster decay pathway, analogous to aggregates in solution. For example, regioregular poly(3-alkyl)thiophenes (P3ATs) have a large triplet yield in solution ($\Phi_T = 0.77$),[38] but do not readily form triplets in a film.[44] Formation of triplet states in the solid state is

(42) Wilson, J. S.; Chawdhury, N.; Al-Mandahary, M. R. A.; Younus, M.; Khan, M. S.; Raithby, P. R.; Köhler, A.; Friend, R. H. *J. Am. Chem. Soc.* **2001**, *123*, 9412–9417.
(43) Liao, L. S.; Fung, M. K.; Lee, C. S.; Lee, S. T.; Inbasekaran, M.; Woo, E. P.; Wu, W. W. *Appl. Phys. Lett.* **2000**, *76*, 3582–3584.
(44) Jiang, X. M. Ö., R.; Korovyanko, O.; An, C. P.; Horovitz, B.; Janssen, R. A. J.; Vardeny, Z. V. *Adv. Funct. Mater.* **2002**, *12*, 587–597.

Table 4. Device Parameters: F8TZPt:PCBM and Pt-T1:PCBM Blend Photovoltaic Devices and SCLC Hole Mobility

active layer	V_{oc}	J_{sc}	FF	η	μ_h(SCLC)
F8TZPt:PCBM	0.38 V	3.5 mA cm^{-2}	0.30	0.40%	2.5×10^{-9} cm^2 $V^{-1}s^{-1}$
Pt-T1:PCBM	0.65 V	5.3 mA cm^{-2}	0.37	1.29%	1.0×10^{-5} cm^2 $V^{-1}s^{-1}$

disfavored for P3ATs in part because the formation of more delocalized, lower energy excimers is more favorable.[45] Formation of triplet excitons in P3AT films is also partly disfavored as a result of decreased twisting between adjacent thiophene units; an increased twist angle between adjacent thiophenes leads to increased spin−orbit coupling.[46] Given that spin−orbit coupling is dominated by the platinum atom in both **F8TZPt** and **Pt-T1**, the change in triplet formation from solution to solid state in **F8TZPt** and **Pt-T1** (as evidenced by singlet oxygen generation) should be primarily the result of lower-energy excimers forming in the polymer films and not a decrease in twisting between adjacent thiophene units. Together, these results suggest that polymers with excitons centered on molecular orbitals with significant contribution from a heavy atom and with lowered aggregation in the solid state would be desirable to generate triplet excitons in a film for photovoltaic devices.

Photovoltaic Devices and Charge Mobility. The polymers **Pt-T1** and **F8TZPt** were studied in bulk heterojunction photovoltaic devices with PCBM to better understand the influence of the cyclometalated platinum moiety on performance. The optimal blending ratio for both **F8TZPt** and **Pt-T1** was found to be 1:4 (polymer:PCBM). Results optimized for polymer:PCBM ratio, thickness, and annealing give power conversion efficiencies of 0.40% for **F8TZPt**, and 1.29% for **Pt-T1** under AM 1.5 illumination at 100 mW cm^{-1}. Figure 6 shows the performance of the devices without annealing. Thermal annealing was found to significantly decrease the performance of the devices, presumably as a result of excessive phase segregation between polymer and PCBM. For **F8TZPt** the J_{sc} is 3.5 mA cm^{-2}, the V_{oc} is 0.38 V, and the fill factor is 0.30. For **Pt-T1** the J_{sc} is 5.3 mA cm^{-2}, the V_{oc} is 0.65 V, and the fill factor is 0.37. The performance

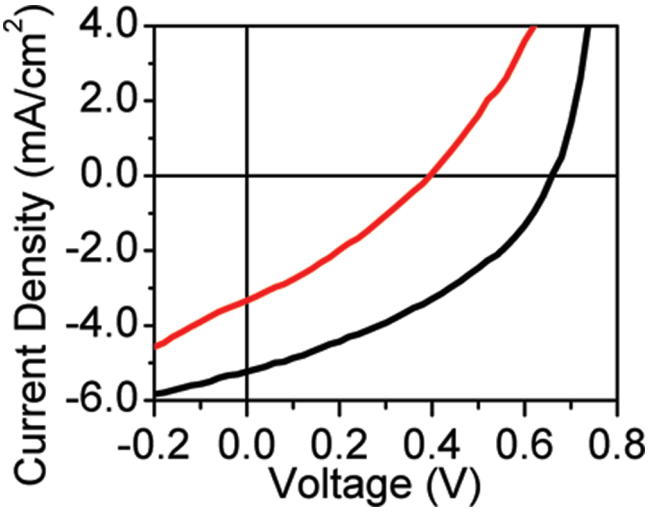

Figure 6. Photovoltaic Performance of **F8TZPt** (red) and **Pt-T1** (black) under AM 1.5 illumination.

of **Pt-T1** is significantly better than **F8TZPt**, which is partly the result of its superior overlap with the solar spectrum. Based on the electrochemistry described previously, it is also possible that holes localize at the platinum unit of **F8TZPt** and this localization inhibits charge transport in a device. The HOMO of **4** is higher than the HOMO of **F8TZPt**, suggesting that the platinum-containing monomer may act as a local energy minimum for holes in the device.

In order to better understand potential limiting factors on photovoltaic performance of polymers containing the cyclometalated platinum complex, the space charge limited current (SCLC) mobilities of **Pt-T1** and **F8TZPt** were measured. Unlike FETs, SCLC mobility determines charge mobility in the vertical direction under no gate bias, making it potentially a more relevant measurement of charge mobility in the context of photovoltaic devices. The zero-field hole mobility of **F8TZPt** is 2.5×10^{-9} cm^2 $V\ s^{-1}$. The inefficient charge transport measured for this polymer clearly contributes to its poor photovoltaic performance, and further suggests that the platinum complex may act as a charge and energy trap in this polymer in which the platinum complex is copolymerized with the wider bandgap fluorene unit. In contrast, the zero-field hole mobility of **Pt-T1** was measured as 1×10^{-5} cm^{-2} V^{-1} s^{-1}. The SCLC mobilities for the pristine polymers and the bulk heterojunction photovoltaic device parameters are summarized in Table 4. The striking difference in SCLC hole mobility between **Pt-T1** and **F8TZPt** demonstrates that comonomer selection may affect both charge transport and photophysics of the resulting polymer. The SCLC hole mobility of **Pt-T1** is lower than that of polythiophenes[47,48] (10^{-4} to 10^{-3} cm^2 V^{-1} s^{-1}), but higher than the reported SCLC hole mobilities of polyplatinynes[7] (10^{-8} to 10^{-7} cm^2 $V^{-1}s^{-1}$). The improved SCLC hole mobility observed for **Pt-T1** relative to the polyplatinynes shows that platinum-containing conjugated polymers with connectivity via a *C^N* ligand are an attractive alternative route to organometallic polymers for photovoltaics.

Conclusions

A new approach to low bandgap platinum-containing conjugated polymers based on a platinum monomer with *C^N* and *O^O* diketonate ligands has been investigated. In these materials the platinum atom is attached adjacent to

(45) Ohkita, H.; Cook, S.; Astuti, Y.; Duffy, W.; Tierney, S.; Zhang, W.; Heeney, M.; McCulloch, I.; Nelson, J.; Bradley, D. D. C.; Durrant, J. R. *J. Am. Chem. Soc.* **2008**, *130*, 3030–3042.
(46) Beljonne, D.; Shuai, Z.; Pourtois, G.; Bredas, J. L. *J. Phys. Chem. A* **2001**, *105*, 3899–3907.
(47) Thompson, B. C.; Kim, B. J.; Kavulak, D. F.; Sivula, K.; Mauldin, C.; Fréchet, J. M. J. *Macromolecules* **2007**, *40*, 7425–7428.
(48) Huang, Y.; Wang, Y.; Sang, G.; Zhou, E.; Huo, L.; Liu, Y.; Li, Y. *J. Phys. Chem. B* **2008**, *112*, 13476–13482.

the conjugated backbone, and therefore does not inhibit exciton delocalization along the polymer chain, providing a means to study the effect of a heavy atom on diffuse excitons. Photovoltaic devices fabricated from these materials yield efficiencies approaching 1.3%, demonstrating that cyclometalated platinum polymers are an attractive new class of materials for organic photovoltaics. Photophysical studies indicate that for some materials long wavelength excitations experience rapid nonradiative decay leading to no observable triplet exciton formation, while other materials exhibit localization of an initially delocalized exciton. This localization promotes triplet formation but is disadvantageous to charge transport in a photovoltaic device. The results presented here suggest that the development of conjugated materials having both significant triplet yields and overlap with the visible spectrum in the solid state will require new materials designed to minimize nonradiative decay pathways at longer excitation wavelengths.

Acknowledgment. This work was supported by the Director, Office of Science, Office of Basic Energy Sciences, Materials Sciences and Engineering Division, of the U.S. Department of Energy under Contract No. DE-AC02-05CH11231. We also thank Thomas W. Holcombe and Jill Millstone for helpful discussions.